General Disclaimer

One or more of the Following Statements may affect this Document

- This document has been reproduced from the best copy furnished by the organizational source. It is being released in the interest of making available as much information as possible.

- This document may contain data, which exceeds the sheet parameters. It was furnished in this condition by the organizational source and is the best copy available.

- This document may contain tone-on-tone or color graphs, charts and/or pictures, which have been reproduced in black and white.

- This document is paginated as submitted by the original source.

- Portions of this document are not fully legible due to the historical nature of some of the material. However, it is the best reproduction available from the original submission.

DOUBLE NODING TECHNIQUE FOR MIXED MODE CRACK PROPAGATION STUDIES

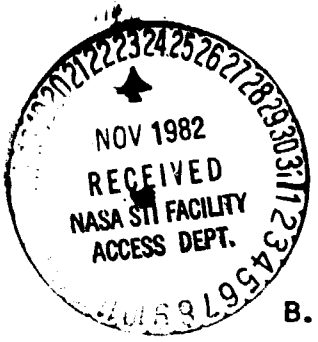

by

B. M. Liaw, A. S. Kobayashi and A. F. Emery

University of Washington
Department of Mechanical Engineering
Seattle, Washington 98195

ABSTRACT

A simple dynamic finite element algorithm for analyzing a propagating mixed mode crack tip is presented. A double noding technique, which can be easily incorporated into existing dynamic finite element codes, is used together with a corrected $\hat{J}$ integral to extract modes I and II dynamic stress intensity factors of a propagating crack. The utility of the procedure is demonstrated by analyzing test problems involving a mode I central crack propagating in a plate subjected to uniaxial tension, a mixed mode I and II stationary, slanted central crack in a plate subjected to uniaxial impact loading, and a mixed mode I and II extending, slanted single edge crack in a plate subjected to uniaxial tension.

(NASA-CR-169535) DOUBLE NODING TECHNIQUE FOR MIXED MODE CRACK PROPAGATION STUDIES (Washington Univ.) 22 p HC A02/MF A01 CSCL 20K

N83-13491

Unclas
G3/39 01176

INTRODUCTION

Most of the recent numerical studies in dynamic fracture mechanics are restricted to mode I crack propagation with the crack extending along the line of symmetry. Crack extension under such condition can be modeled with finite element method by simply releasing the crack tip node at the line of symmetry following a prescribed nodal force versus crack extension history. Mode I dynamic stress intensity factor in dynamic fracture analysis of isotropic material is justified since the crack will ordinarily propagate in the direction perpendicular to the maximum principal stress direction. There are conditions, however, when the crack will deviate from its self-similar crack extension path to curve [1] or to bifurcate [2] under specific static or dynamic loadings. Such crack extension away from the line of symmetry in a finite element mesh cannot be accomplished by the above-mentioned simple nodal release mechanism. The double-noding [3] and the nodal-grafting [4] techniques are two procedures which have been used to model off-axis crack propagation. While details of the former are not available, the latter requires a higher order isoparametric element in the dynamic finite element code. The double noding technique presented in this paper was developed for use with an implicit dynamic finite element code which utilizes a conventional isoparametric quadrilateral element.

THEORETICAL BACKGROUND

Double Noding Technique

Consider a slanted crack in a two dimensional space with a local x-y coordinate system oriented along the local crack tip region as shown in Figure 1. The dynamic equations of motion for the crack tip element with nodal displacements of $\{q\}$, nodal velocities of $\{\dot{q}\}$, nodal accelerations of

$\{\ddot{q}\}$, nodal forces of $\{F\}$, stiffness of $[K]$ and mass matrix of $[M]$ are:

$$[K]\{q\} + [M]\{\ddot{q}\} = \{F\} \tag{1}$$

If the ith and jth degrees of freedom in the above displacements, velocities and accelerations are constrained to be equal

$$q_i = q_j, \quad \dot{q}_i = \dot{q}_j, \quad \ddot{q}_i = \ddot{q}_j \tag{2}$$

through double noding, then define the relative displacement $\{q'\}$ as

$$\{q\} = [T] \{q'\}, \text{ etc.} \tag{3}$$

$$\{F'\} = [T]^T\{F\} \tag{4}$$

where T_{mn} = 1 when m = n

= 1 when m = i and m = j

= 0 all other m and n

and

$$q'_i = q_i - q_j = 0 \quad \text{when } k = i$$

$$q'_k = q_k \qquad \text{when } k \neq i \tag{5}$$

Substituting Equations (3), (4) and (5) into Equation (1) yields

$$[K']\{q'\} + [M']\{\ddot{q}'\} = \{F\}$$
$$= [T]^T\{F\}$$
$$= [T]^T[K]\{q\} + [T]^T[M]\{\ddot{q}\}$$
$$= [T]^T[K][T]\{q'\} + [T]^T[M][T]\{\ddot{q}'\} \quad (6)$$

The equivalent stiffness and mass matrices in the above equivalent dynamic equations of motion are

$$[K'] = [T]^T[K][T] \quad (7)$$

$$[M'] = [T]^T[M][T] \quad (8)$$

Equations (3) through (8) constitutes the equivalent system for the slanted crack with two and more degrees of freedom constrained by the double noded current and future crack tip nodes. The equivalent nodal displacements are determined by applying Newmark's beta method to the dynamic equations of motion. The nodal displacements at the double nodes are then determined by Equation (3).

Nodal Force Release

Crack extension with a traction free crack surface requires elimination of the nodal forces normal, $F_{2\ell}$ and F_{2r}, and tangential, $F_{1\ell}$ and F_{1r}, to the crack surface as shown in Figure 1. The crack tip nodal force components are released simultaneously in equal increments to model a linear translation of the crack tip to its new crack tip node, $(\bar{F}_{1r}, \bar{F}_{1\ell}, \bar{F}_{2r}, \bar{F}_{2\ell}) = (\bar{F}_{1r}, \bar{F}_{1\ell}, \bar{F}_{2r}, \bar{F}_{2\ell})(1-\frac{\Delta}{d})$, where bar denotes the forces at the double node prior to crack extension, Δ is the current crack tip location and d is the crack

distance to its adjacent node. Details of this release procedure as well as its comparison with others are described in Reference [5].

$\hat{J}$ Integral

The corrected $\hat{J}$ integral was used to determine the modes I and II dynamic stress intensity factors, K_I and K_{II}, respectively. The $\hat{J}$ integral as defined by Kishimoto et al [6] is

$$\hat{J} + \int_{\Gamma} [Wn_1 - T_i u_{i,1}] d\Gamma + \int_A \rho \ddot{u}_i u_{i,1} dA \qquad (9)$$

where the indices refer to the local x_1 and x_2 coordinates shown in Figure 1, W is the strain energy density, n_1 is the surface normal to the integration path Γ_1 and ρ is the density.

By taking a symmetric integration path with respect to the crack extension direction, as shown in Figure 1, the $\hat{J}$ integral, which contains both K_I and K_{II}, can be decomposed into two path-independent integrals $\hat{J}_I$ and $\hat{J}_{II}$ as

$$\hat{J} = \hat{J}_I + \hat{J}_{II} \qquad (10)$$

where $\hat{J}_I$ and $\hat{J}_{II}$ are only functions of K_I and K_{II}, respectively. Detailed formulations of $\hat{J}_I$ and $\hat{J}_{II}$ are described by Kishimoto et al. [6].
For a stationary crack, Ishikawa et al [7] has shown that

$$\hat{J}_I = \frac{\kappa+1}{8\mu} K_I^2 \qquad (11a)$$

$$\hat{J}_{II} = \frac{\kappa+1}{8\mu} K_{II}^2 \qquad (11b)$$

where $\kappa = \begin{cases} 3 - 4\nu & \text{plane strain} \\ \dfrac{3-\nu}{1+\nu} & \text{plane stress} \end{cases}$

and μ and ν are the shear modulus and Poisson's ratio, respectively.

For a propagating crack, Atluri et al. [8,9] has shown that

$$\hat{J}_I = \frac{\hat{F}_I(\dot{a})}{2\mu} K_I^2 \qquad (12a)$$

$$\hat{J}_{II} = \frac{\hat{F}_{II}(\dot{a})}{2\mu} K_{II}^2 \qquad (12b)$$

where $\hat{F}_I(\dot{a}) = \frac{S_1(1-S_2^2)}{D^2}\left[2S_1(1+S_2) - \frac{(1+S_1)}{2S_1}(1+S_2^2)^2 - 2(S_1-S_2)\frac{(1+S_2^2)^2}{\sqrt{(1+S_1)(1+S_2)}}\right]$ (12c)

$$\hat{F}_{II}(\dot{a}) = \frac{S_2(1-S_2^2)}{D^2}\left[2S_2(1+S_1) - \frac{(1+S_2)}{2S_2}(1+S_2^2)^2 - 2(S_2-S_1)\frac{(1+S_2^2)^2}{\sqrt{(1+S_1)(1+S_2)}}\right] \qquad (12d)$$

$$S_1^2 = 1 - \left(\frac{\dot{a}}{C_1}\right)^2 \qquad S_2^2 = 1 - \left(\frac{\dot{a}}{C_2}\right)^2 \tag{12e}$$

$$D = 4S_1S_2 - (1+S_2^2)^2 \tag{12f}$$

and $\dot{a}$, C_1 and C_2 are the crack velocity, dilatational and distortional stress wave velocities, respectively.

NUMERICAL PROCEDURE

The numerical procedure consists of inputting the above double noding technique to an implicit dynamic finite element code and releasing the crack tip nodal force linearly in accordance with a prescribed crack tip motion. As shown by Equations (12), the associated dynamic stress intensity factors, K_I and K_{II}, can be determined by numerically evaluating the $\hat{J}_I$ and $\hat{J}_{II}$ integrals along predetermined symmetric contours surrounding the instantaneous crack tip. Separation of the $\hat{J}$ integral of Equation (10) into the two $\hat{J}_I$ and $\hat{J}_{II}$ integrals is accomplished by using the decomposition procedure initially developed by Ishikawa et al. [7] for a static mixed mode crack and which was later extended to a dynamically loaded mixed mode crack by Kishimoto et al. [6]. The procedure consists of first decomposing the displacements, strains, stresses and body forces into symmetric and anti-symmetric components after which Equation (9) is used to compute $\hat{J}_I$ and $\hat{J}_{II}$ integrals, respectively. In the following, three problems which utilize the above mentioned double noding technique together with the $\hat{J}_I$ and $\hat{J}_{II}$ integral technique of determining K_I and K_{II} are described. The examples involved

steel plate under a plane strain state of stress with material properties of $\mu = 2.94 \times 10^{10}$ N/m^2, $\nu = 0.286$ and $\rho = 2.45 \times 10^3$ Kg/m^3.

EXTENDING CENTRAL CRACK IN A PLATE SUBJECTED TO UNIAXIAL TENSION

The Broberg problem [10] of a central crack extending at constant velocity in a uniaxial tension field has been used by many to verify their dynamic finite element codes. This problem yields only a mode I dynamic stress intensity factor, but it offers the only comparison between results generated by other dynamic finite element codes. Figure 2 shows the finite element break down of a half-plane as well as the seven integration paths used in this analysis. The complete specimen geometry is shown in the legend of Figure 3. Variations in the numerically determined mode I dynamic stress intensity factors with the integration paths for five crack tip locations of $a/W = 0.2$, 0.3, 0.4, 0.5 and 0.6 and three crack velocities of $\dot{a}/C_2 = 0$, 0.2 and 0.6 are shown in Table 1, where a is the half crack length and W is the half plate width. Maximum difference of 1 percent between the K_I computed for the various integration paths shows that the path independency is satisfied for all practical purpose.

Figure 3 shows the changes in the static and the dynamic stress intensity factors for two dynamic crack velocities. Also shown for comparison purpose are the static results of Isida [11] and the two dynamic results of Nishioka and Atluri [12,13]. The 13 percent lower K_I at the shorter crack length of $a/W = 0.25$ at a higher crack velocity of $\dot{a}/C_2 = 0.6$ is due in part to the coarser and conventional element used in this analysis. Otherwise, good agreements between the various results are noted.

STATIONARY SLANTED CENTRAL CRACK IN A PLATE SUBJECTED TO UNIAXIAL IMPACT

LOADING

Mixed mode dynamic stress intensity factors in a stationary slanted central crack in a plate subjected to uniaxial impact loading of $\sigma H(t)$ was first analyzed by Thau and Lu [14] using Wiener-Hopf technique and by Kishimoto et al. [6] using finite element analysis. This problem was also analyzed in this paper in order to compare the applicability of present finite element algorithm with the above known results. Figure 4 shows the finite element break down and the five integration paths used in this analysis. Table 2 shows the variations in the normalized K_I and K_{II} at four time intervals of the stationary crack. While the differences in K_{II} for the five integration paths is as high as 8 percent, the relatively small K_{II} values makes this difference insignificant. Figure 5 shows changes in transient K_I and K_{II} with time for the stationary crack where R_0, R_1, R_2 denoting the first arrival times at the crack tip for incident wave from leading edge, the reflected waves from upper/lower boundaries and the reflected wave from the rear edge, respectively. While agreements between the three results for the stationary crack is good at the initial stage, the finite element results differ towards the latter part of time interval of 14 $\sim$ 20 s. Equally puzzling is the large differences between the static stress intensity factors for the plate under static loading by these two finite element analyses. Such discrepancy may result from different finite element mesh and geometry (triangular versus quadrilateral) by Kishimoto et al. [6] and by the present computation. Nevertheless, the general results of these two analyses are very similar.

EXTENDING SLANTED SINGLE EDGE CRACK IN A PLATE SUBJECTED TO UNIAXIAL TENSION

As a further study in mixed mode dynamic crack, an extending slanted

single edge crack in a plate subjected to uniaxial tension, which is the dynamic counterpart of the static solution of Bowie [15], was analyzed. This crack was extended along its original crack direction at two crack velocities of $\dot{a}/C_2$ = 0.2 and 0.6. Figure 6 shows the finite element breakdown as well as the four integration paths used in this analysis. Table 3 shows the variations in K_I and K_{II} at five crack tip locations for the static and two propagating cracks. Unlike the previous case, little variation in K_{II} are noted, possibly due to the relatively larger values of K_{II} in this problem. Figure 7 shows the changes in K_I and K_{II} with crack extension. Also shown for comparison is the static results of Bowie [15] which are within 4% of the present analysis. While one would not expect self-similar crack propagation under this loading condition, it is interesting to note the closeness of K_I and K_{II} values at the higher crack velocity of $\dot{a}/C_2$ = 0.6.

CONCLUSIONS

A double noding technique suitable for dynamic finite element analysis of a crack extending under mixed mode loading condition is presented. Mixed mode dynamic stress intensity factors are computed by using the $\hat{J}$ integrals as modified by Atluri et al. [8,9] for the extending crack.

The procedure was used to determine the dynamic stress intensity factors of an extending central crack in a uniaxially loaded plate, the dynamic stress intensity factors of a stationary slanted central crack in an uniaxially impacted plate and the static and dynamic stress intensity factors of an extending slanted, single edge crack in a uniaxially loaded plate. The computed values by this procedure were generally in good agreement with known results.

When modified by appropriate criteria of dynamic crack curving [1] and

branching [2], this simple procedure can be used to determine the dynamic fracture parameters associated with such problems.

ACKNOWLEDGEMENT

This investigation was supported by NASA Grant NGL 48-002-004 to the Ceramic Engineering Division, University of Washington. The authors express their gratitude to Professor J. I. Mueller, Principal Investigator of the Ceramic Material Research Program for his continuing support over the past four years.

REFERENCES

1. Ramulu, M. and Kobayashi, A. S., "Dynamic Crack Curving - A Photoelastic Evaluation", to be published in Experimental Mechanics.

2. Ramulu, M., Kobayashi, A. S. and Kang, B. S.-J, "Dynamic Crack Branching - A Photoelastic Evaluation", submitted for publication in ASTM STP.

3. Kanninen, M. F., Brust, F. W., Ahmad, J. and Abou-Sayed, I. S., "The Numerical Simulation of Crack Growth in Weld-Induced Residual Stress Fields", to be published in the Proceedings of the 28th Army Sagamore Research Conference.

4. Ingraffea, A. R., "Nodal Grafting for Crack Propagation Studies", International Journal for Numerical Methods in Engineering, vol. 11, 1977, pp 1185 - 1187.

5. Kobayashi, A. S., Seo, K., Jou, J.-Y. and Urabe, Y., "Dynamic Analysis of Homalite-100 and Polycarbonate Modified Compact Tension Specimens", Experimental Mechanics, 20 (3), 1980, pp 73 - 79.

6. Kishimoto, K. Aoki, S. and Sakata, M., "Dynamic Stress Intensity Factors Using J-Integral and Finite Element Method", Engineering Fracture Mechanics, Vol. 13, 1980, pp 387 - 394.

7. Ishikawa, H., Kitagawa, H. and Okamura, H., "J-Integral of a Mixed-Mode Crack and Its Application", Proceedings of the Third International Conference of Mechanical Behaviors of Materials, Vol. 3, 1979, pp 447 - 455.

8. Nishioka, T. and Atluri, S. N., "Path-Independent Integrals, Energy Release Rates, and General Solutions of Near-Tip Fields in Mixed Mode Dynamic Fracture Mechanics", to be published in Engineering Fracture Mechanics.

9. Atluri, S. N., "Path-Independent Integrals in Finite Elasticity and Inelasticity with Body Forces, Inertia and Arbitrary Crack-Face Conditions", Engineering Fracture Mechanics, 16 (3), 1982, pp 341 -364.

10. Broberg, K. B., "The propagation of a brittle crack", Arkiv for Fysik, 13 (10), 1960, pp 159 - 192.

11. Ishida, M., "Analysis of stress intensity factors for the tension of a centrally cracked strip with stiffened edges", Engineering Fracture Mechanics, 5 (3), September 1973, pp 647 - 665.

12. Nishioka, T. and Atluri, S. N., "Numerical Modeling of Dynamic Crack Propagation in Finite Bodies, by Moving Singular Elements, Part I: Formulation", ASME Journal of Applied Mechanics, 102 (3), 1980, pp 570 - 576.

13. Nishioka, T. and Atluri, S. N., "Numerical Modeling of Dynamic Crack Propagation in Finite Bodies, by Moving Singular Elements, Part II: Results", ASME Journal of Applied Mechanics, 102 (3), 1980, pp 577 - 583.

14. Thau, S. A. and Lu, T. H., "Transient Stress Intensity Factors for a Finite Crack in an Elastic Solids Caused by a Dilatational Wave", International Journal of Solids and Structures, 7, 1971, pp. 731-750.

15. Bowie, O. L., "Solutions of plane crack problems by mapping technique", Mechanics of Fracture I, Methods of analysis and solutions of crack problems, ed. by G. C. Sih, Noordhoff International Publishing, Leyden, 1973, pp. 1-55.

TABLE 2.
PATH INDEPENDENCE OF $\hat{J}$-INTEGRAL FOR
EXTENDING CENTRAL CRACK PROBLEM

		$K_I/\sigma\sqrt{\pi W}$						
$\dot{a}/C_2$	a/W	Path 1	2	3	4	5	6	7
0	0.2	0.4530	0.4602	0.4607	0.4593	0.4582	0.4576	0.4571
	0.3	0.5974	0.5987	0.6008	0.6012	0.5999	0.5988	0.5978
	0.4	0.7493	0.7500	0.7514	0.7526	0.7516	0.7500	0.7485
	0.5	0.8316	0.8325	0.8339	0.8350	0.8338	0.8319	0.8302
	0.6	0.9195	0.9207	0.9223	0.9230	0.9211	0.9188	0.9170
0.2	0.3	0.4560	0.4617	0.4617	0.4620	0.4606	0.4601	0.4597
	0.4	0.5630	0.5702	0.5713	0.5690	0.5701	0.5682	0.5673
	0.5	0.7278	0.7335	0.7318	0.7281	0.7310	0.7286	0.7275
	0.6	0.9099	0.9251	0.9215	0.9108	0.9144	0.9108	0.9103
0.6	0.3	0.2459	0.2487	0.2553	0.2598	0.2588	0.2580	0.2574
	0.4	0.2951	0.3098	0.3084	0.3079	0.3106	0.3097	0.3088
	0.5	0.3423	0.3572	0.3583	0.3558	0.3556	0.3563	0.3569
	0.6	0.3703	0.3878	0.3889	0.3881	0.3878	0.3869	0.3860

a is the half crack length.
W is the half plate width.
σ is the applied uniaxial load.

TABLE 2
PATH INDEPENDENCE OF $\hat{J}$ INTEGRAL FOR
STATIONARY SLANTED CENTRAL CACK PROBLEM

	$K_I/\sigma\sqrt{\pi W}$					$K_{II}/\sigma\sqrt{\pi W}$				
TIME	Path 1	2	3	4	5	Path 1	2	3	4	5
5μs	0.1625	0.1619	0.1616	0.1615	0.1596	0.0825	0.0857	0.0895	0.0896	0.0888
10	[illegible]706	0.3730	0.3740	0.3711	0.3686	0.2837	0.2833	0.2776	0.2770	0.2809
15	1.0422	1.0492	1.0552	1.0532	1.0512	0.6190	0.6171	0.6089	0.6067	0.6050
20	1.1699	1.1769	1.1779	1.1729	1.1739	0.8234	0.8190	0.8092	0.8071	0.8098

W is the half plate width.
σ is the applied uniaxial impact load intensity.

TABLE 3
PATH INDEPENDENCE OF $\hat{J}$ INTEGRAL FOR
EXTENDING SLANTED SINGLE EDGE CRACK PROBLEM

		$K_I/\sigma\sqrt{\pi W}$				$K_{II}/\sigma\sqrt{\pi W}$			
		Path				Path			
$\dot{a}/C_2$	a/W	1	2	3	4	1	2	3	4
	0.2	0.4314	0.4437			0.2243	0.2220		
	0.3	0.6583	0.6638	0.6726	0.6691	0.3226	0.3212	0.3198	0.3270
0	0.4	1.0079	1.0111	1.0167	1.0245	0.4498	0.4485	0.4455	0.4405
	0.5	1.5784	1.5829	1.5897	1.5972	0.6134	0.6102	0.6036	0.5865
	0.6	2.5244	2.5451	2.5226	2.5223	0.8462	0.8230	0.7749	0.7488
	0.3	0.4205	0.4252	0.4316	0.4254	0.2708	0.2708	0.2708	0.2749
	0.4	0.5497	0.5550	0.5563	0.5613	0.3122	0.3111	0.3099	0.3108
0.2	0.5	0.7549	0.7590	0.7583	0.7627	0.4163	0.4168	0.4167	0.4142
	0.6	0.8831	0.9010	0.8902	0.9001	0.5579	0.5387	0.5227	0.5263
	0.3	0.1762	0.1863	0.1914	0.1774	0.2166	0.2178	0.2161	0.2252
0.6	0.4	0.2095	0.2240	0.2187	0.2190	0.2287	0.2322	0.2360	0.2326
	0.5	0.2211	0.2347	0.2321	0.2351	0.2661	0.2648	0.2641	0.2639
	0.6	0.2571	0.2793	0.2750	0.2759	0.2282	0.2834	0.2772	0.2783

a is the crack length.
W is the plate width.
σ is the applied uniaxial load.

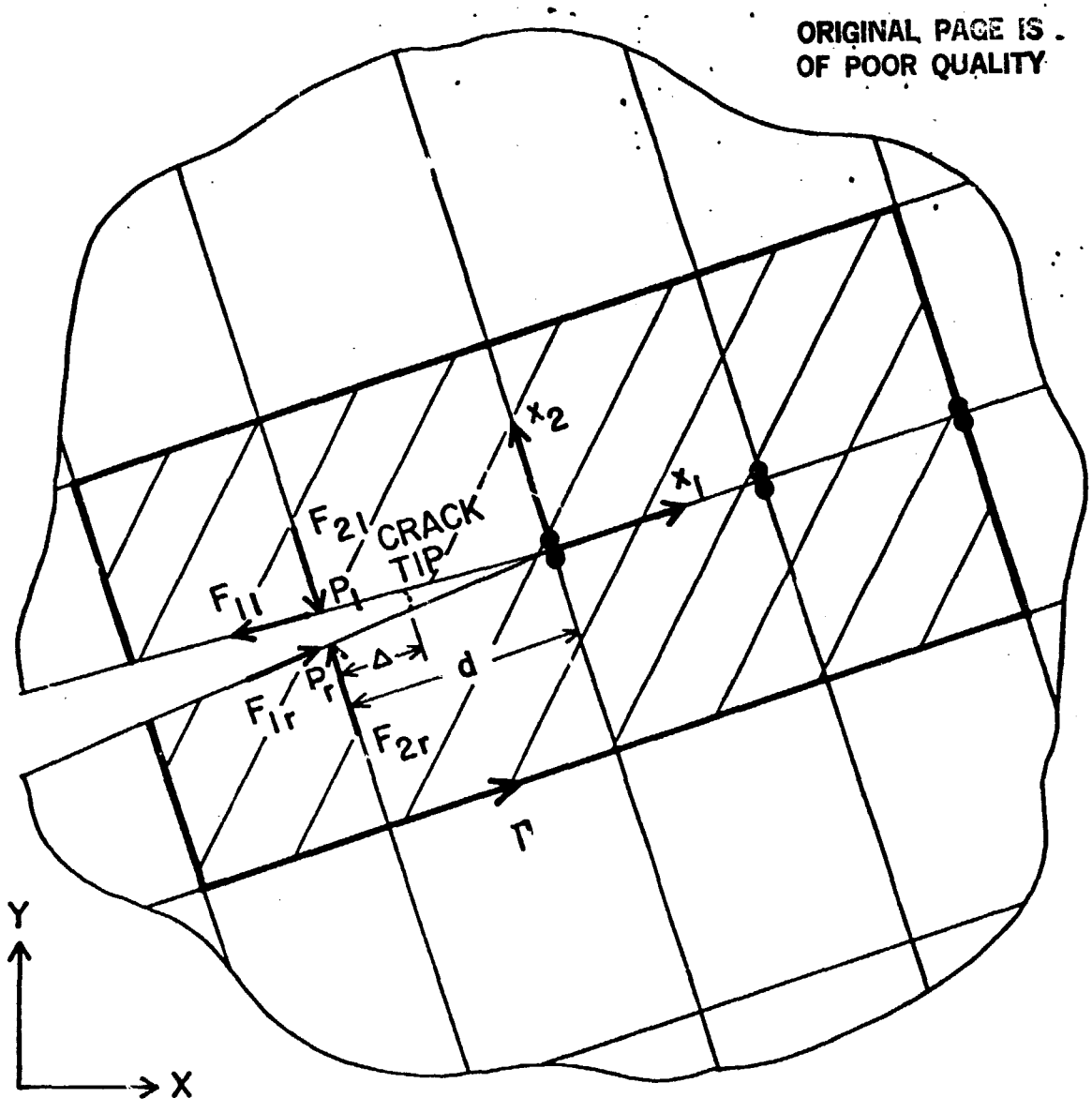

● Double Nodes

FIGURE 1. DOUBLE NODING, NODAL FORCE RELEASE AND $\hat{J}$ INTEGRAL PATH, Γ.

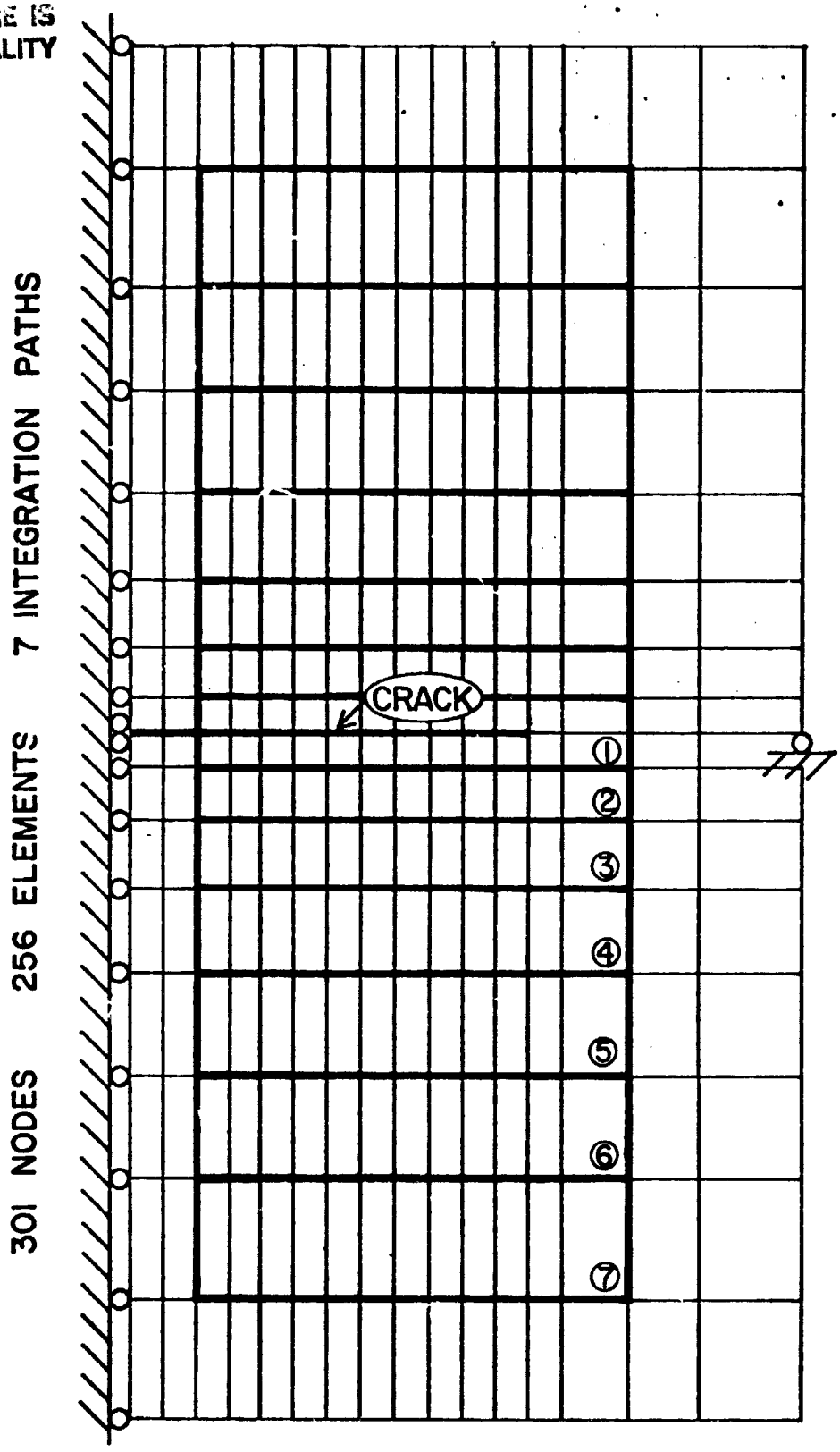

FIGURE 2. FINITE ELEMENT BREAKDOWN OF A HALF PLANE OF AN EXTENDING CENTRAL CRACK.

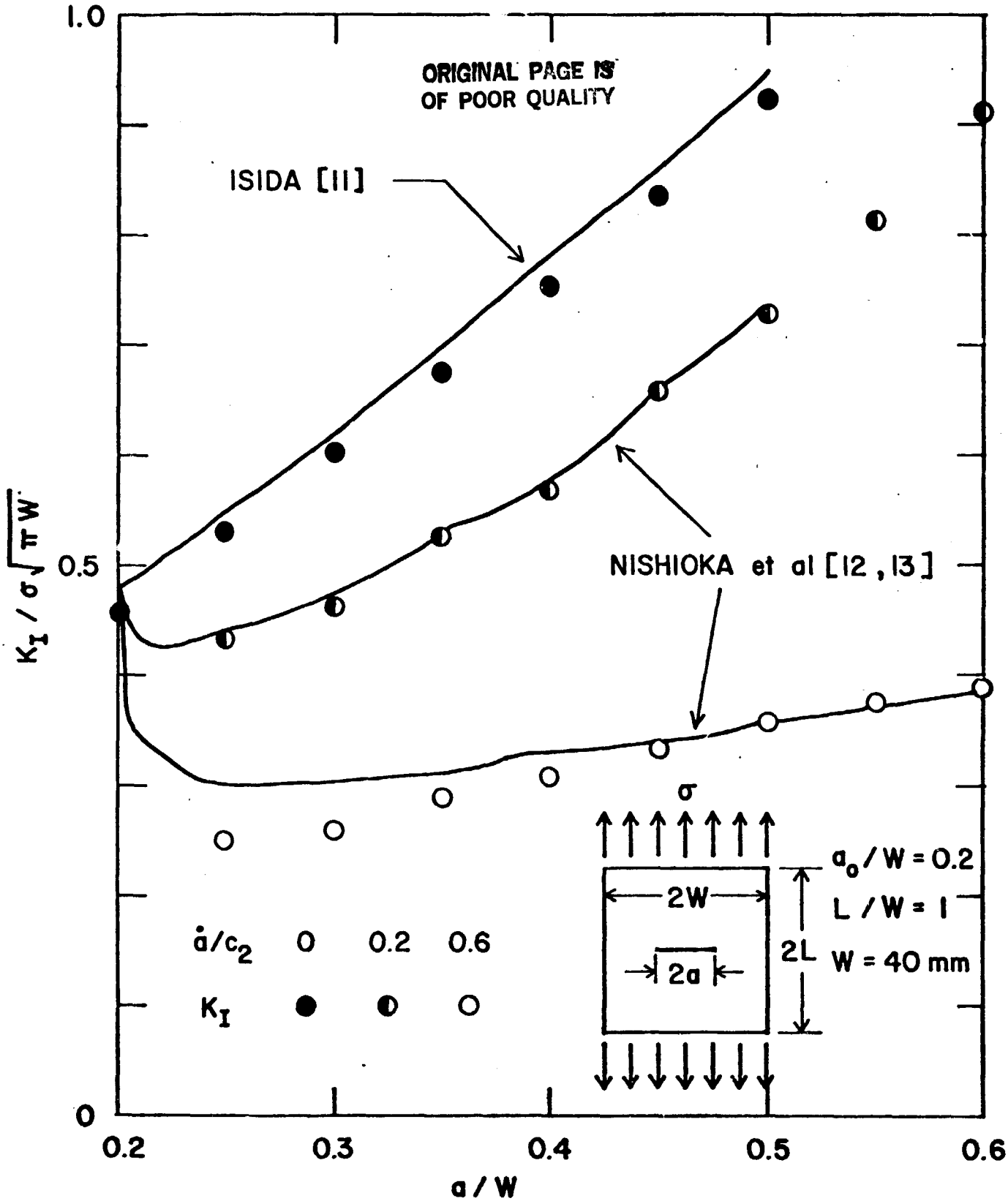

FIGURE 3. NORMALIZED STRESS INTENSITY FACTORS OF EXTENDING CENTRAL CRACK.

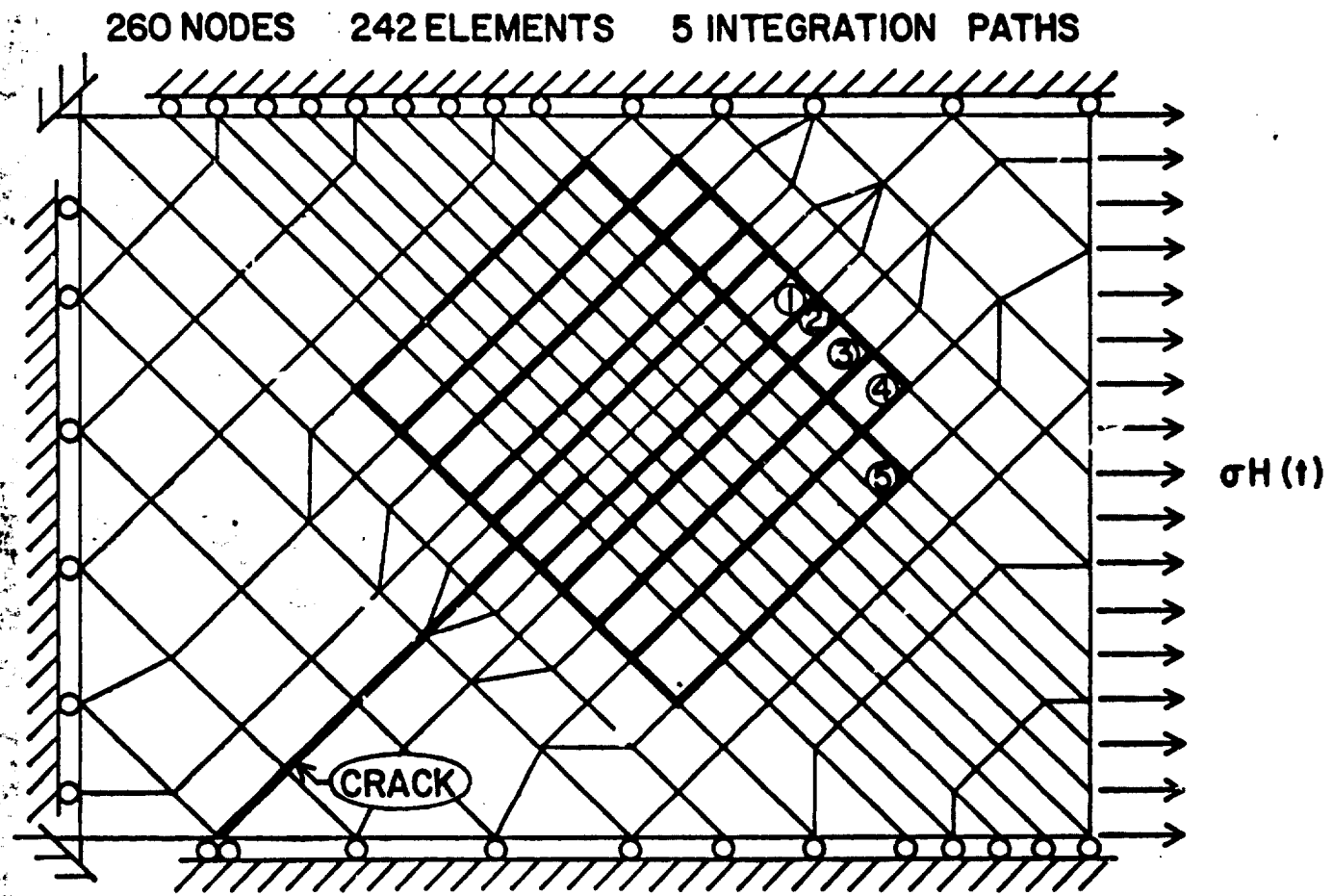

FIGURE 4. FINITE ELEMENT BREAKDOWN OF STATIONARY SLANTED CENTRAL CRACK.

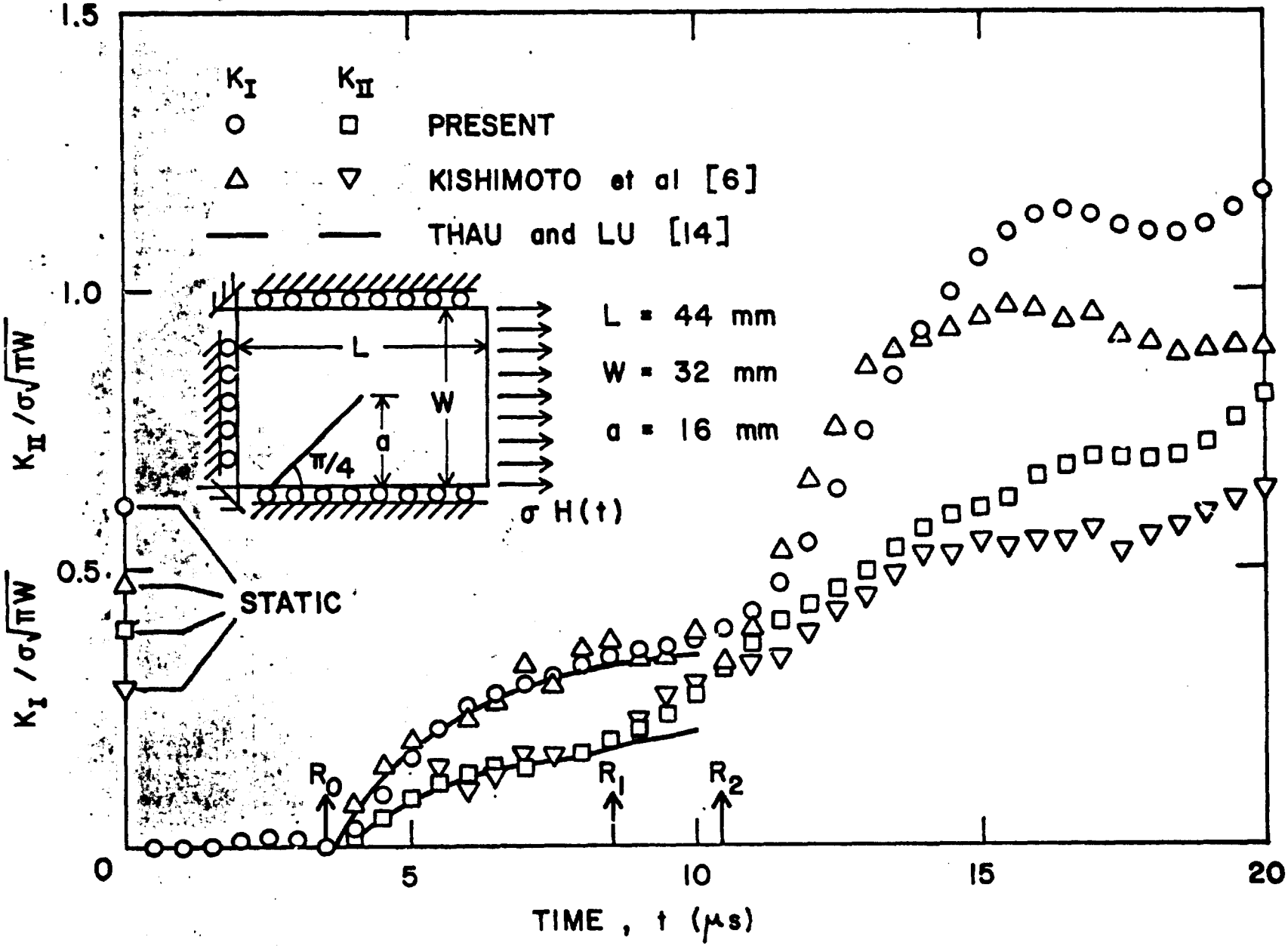

FIGURE 5. NORMALIZED DYNAMIC STRESS INTENSITY FACTORS OF STATIONARY SLANTED CENTRAL CRACK.

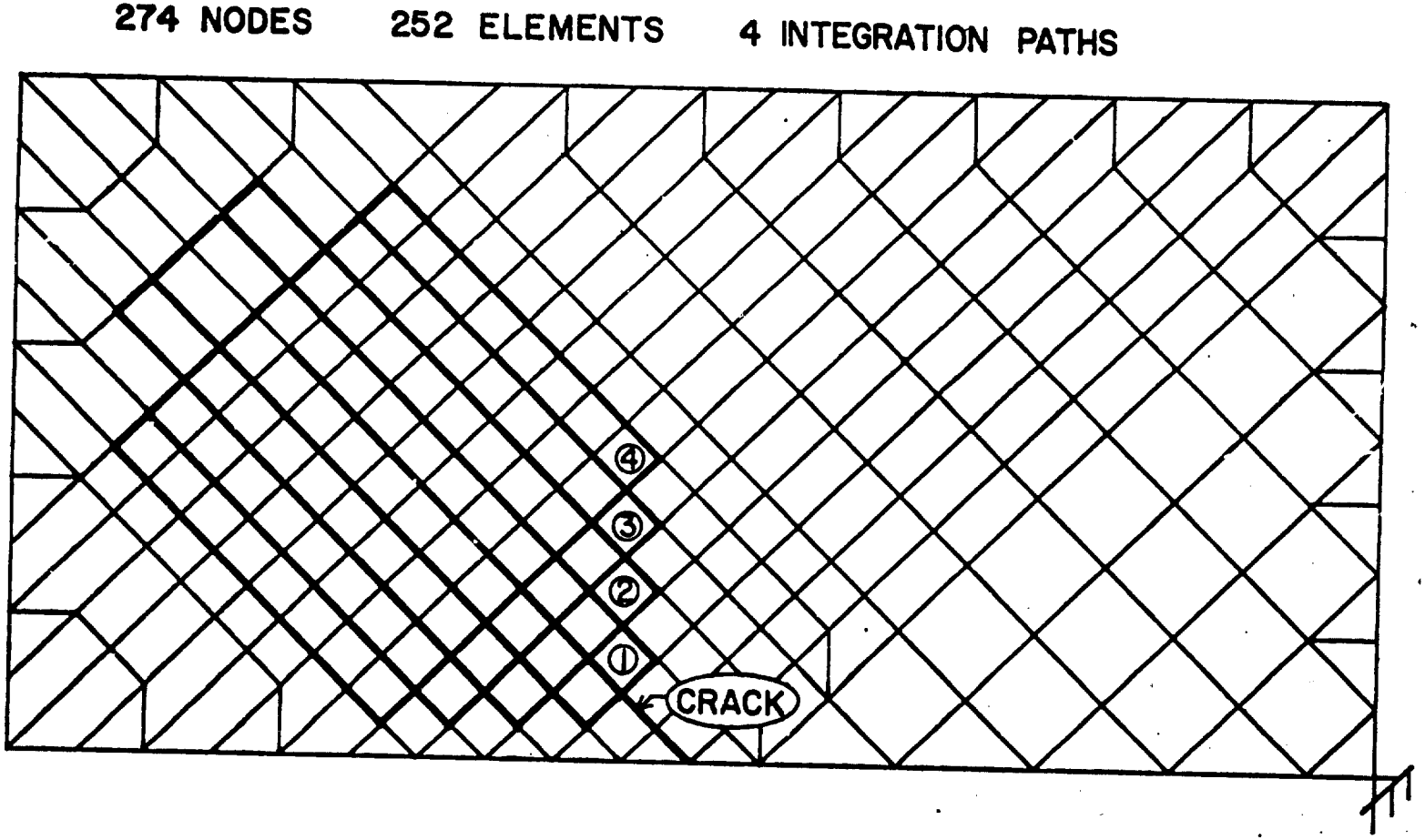

ORIGINAL PAGE IS
OF POOR QUALITY

FIGURE 6. FINITE ELEMENT BREAKDOWN OF EXTENDING SLANTED SINGLE EDGE CRACK.

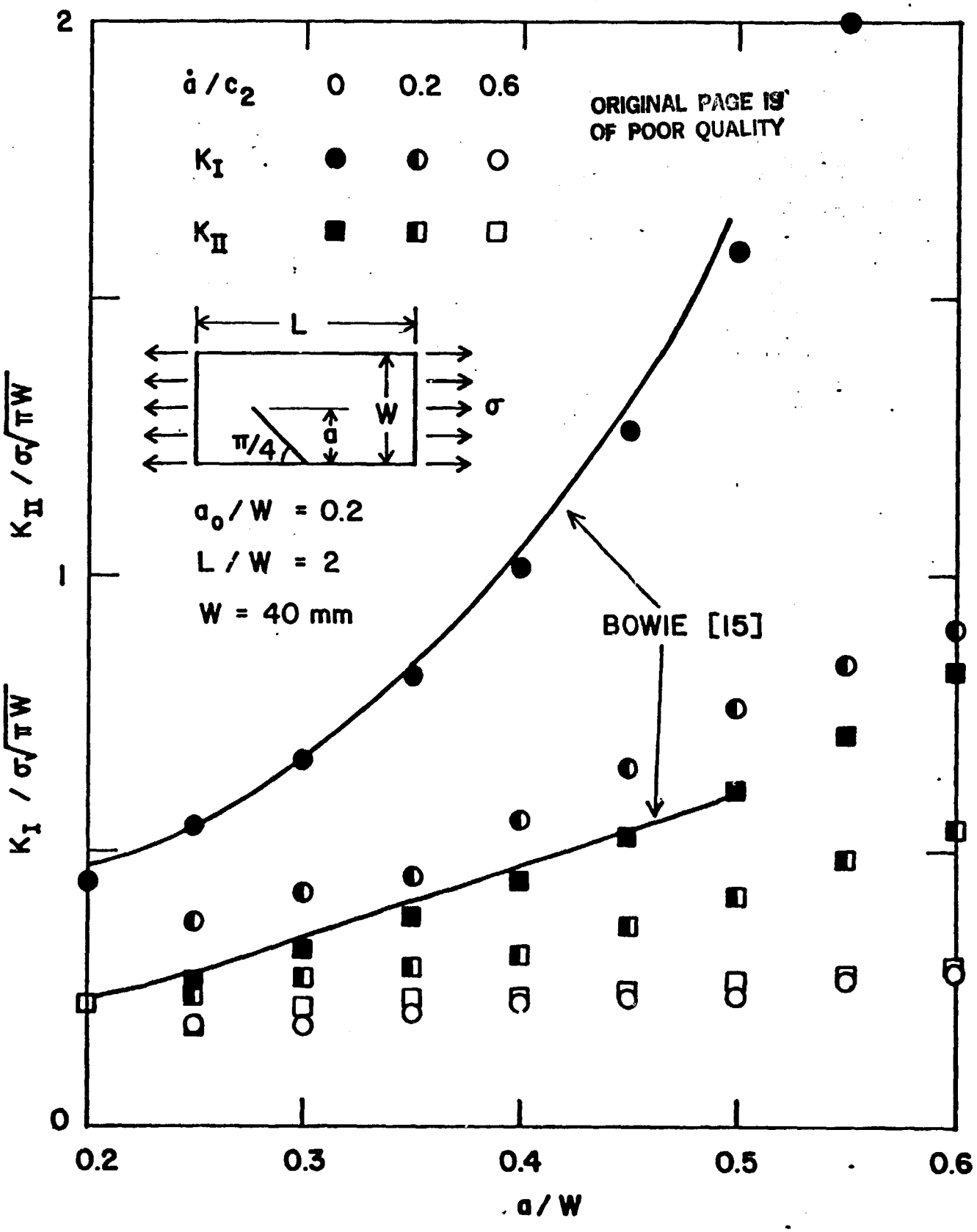

FIGURE 7. NORMALIZED STRESS INTENSITY FACTORS OF EXTENDING SLANTED SINGLE EDGE CRACK.